American Journal of Engineering Research (AJER)
e-ISSN : 2320-0847 p-ISSN : 2320-0936
Volume-02, Issue-11, pp-129-150
www.ajer.org

Research Paper Open Access

Control of Biped Robot with Stable Walking

Tran Dinh Huy, Ngo Cao Cuong, and Nguyen Thanh Phuong
HUTECH High Technology Research Instituite

Abstract: - This paper presents the development results of the 10 DOF biped robot with stable and human-like walking using the simple hardware configuration. Kinematics model of the 10 DOF biped robot and its dynamic model based on the 3D inverted pendulum are presented. Under assumption that the COM of the biped robot moves on the horizontal constraint plane, ZMP equations of the biped robot depending on the coordinate of the center of the pelvis link obtained from the dynamic model of the biped robot are given based on the D'Alembert's principle. A ZMP servo control system is constructed to track the ZMP of the biped robot to ZMP reference input which is decided by the footprint of the biped robot. A discrete time optimal controller is designed to control ZMP of the biped robot to track trajectories reference inputs based on discrete time systems. When ZMP of biped robot is controlled to track trajectory reference input decided inside stable region, a trajectory of COM is generated as stable walking pattern of the biped robot. Based on the stable walking pattern of the biped robot, a stable walking control method of the biped robot is proposed. From the trajectory of COM of the biped robot and trajectory reference input of the swinging leg, inverse kinematics solved by solid geometry method is used to compute the angle of joints of the biped robot. Because joint's angles reference of the biped robot are computed from the stable walking pattern of the biped robot, the walking of the biped robot is stable if the joint's angles of the biped robot are controlled to track those references. The stable walking control method of the biped robot is implemented by simple hardware using PIC18F4431 and dsPIC30F6014. The simulation and experimental results show the effectiveness of this control method.

Keywords: - *Discrete Time Optimal Control, ZMP Servo Control System, Biped Robot.*

I. INTRODUCTION

Research on humanoid robots and biped locomotion is currently one of the most exciting topics in the field of robotics and there exist many ongoing projects. Although some of those works have already demonstrated very reliable dynamic biped walking [12], it is still important to understand the theoretical background of the biped robot. The biped robot performs its locomotion relatively to ground while it is keeping its balance and not falling down. Since there is no base link fixed on the ground or the base, the gait planning and control of the biped robot is very important but difficult. Up so far, numerous approaches have been proposed. The common method of these numerous approaches is to restrict zero moment point (ZMP) within stable region to protect biped robot from falling down [8].

In the recent years, a great amount of scientific and engineering research has been devoted to the development of legged robots able to attain gait patterns more or less similar to human beings. Towards this objective, many scientific papers have been published, focusing on different aspects of the problem. Sunil, Agrawal and Abbas [3] proposed motion control of a novel planar biped with nearly linear dynamics. They introduced a biped robot that the model was nearly linear. The motion control for trajectory following used nonlinear control method. Jong Hyeon Park [4] proposed impedance control for biped robot locomotion so that both legs of the biped robot were controlled by the impedance control, where the desired impedance at the hip and the swing foot was specified. Qiang Huang and Yoshihiko [5] introduced sensory reflex control for humanoid walking so that the walking control consisted of a feedforward dynamic pattern and a feedback sensory reflex. In these papers, the moving of the body of the robot was assumed to be only on the sagittal plane. The biped robot was controlled based on the dynamic model. The ZMP of the biped robot was measured by sensor so that the structure of the biped robot was complex and required high speed controller hardware system. This paper presents a stable walking control of biped robot by using inverse kinematics with simple hardware configuration based on the walking pattern which is generated by ZMP servo system. The robot's body can

move on sagittal and lateral plane. Furthermore, the walking pattern is generated based on the ZMP of the biped robot so that the stable of the biped robot during walking or running is guaranteed without the sensor system to measure ZMP of biped robot. In addition, a simple inverse kinematics using solid geometry is used to obtain angle of joints of the biped robot based on the stable walking pattern. The biped robot is modeled as 3D inverted pendulum [1]. A ZMP servo system is constructed based on the ZMP equation to generate trajectory of center of mass (COM). A discrete time optimal tracking controller is also designed to control ZMP servo system. From the trajectory of COM, inverse kinematics of the biped robot is solved by solid geometry method to obtain angle joints of the biped robot. It is used to control walking of the biped robot.

II. MATHEMATIC MODEL OF THE BIPED ROBOT

2.1 Kinematics Model of Biped Robot

A 10 DOF biped robot developed in this thesis is considered as shown in Fig. 1. It is assumed that the biped robot is supported by right leg and swung by left leg.

In Fig. 1, l_1 and l_5 are length of the lower links of the right leg and left leg, l_2 and l_4 are length of the upper links of the right leg and left leg, l_3 is length of the pelvis link, (x_b, y_b, z_b) and (x_e, y_e, z_e) are coordinates of the ankle joints B_2 and E, and (x_c, y_c, z_c) is coordinate of the center of pelvis link C.

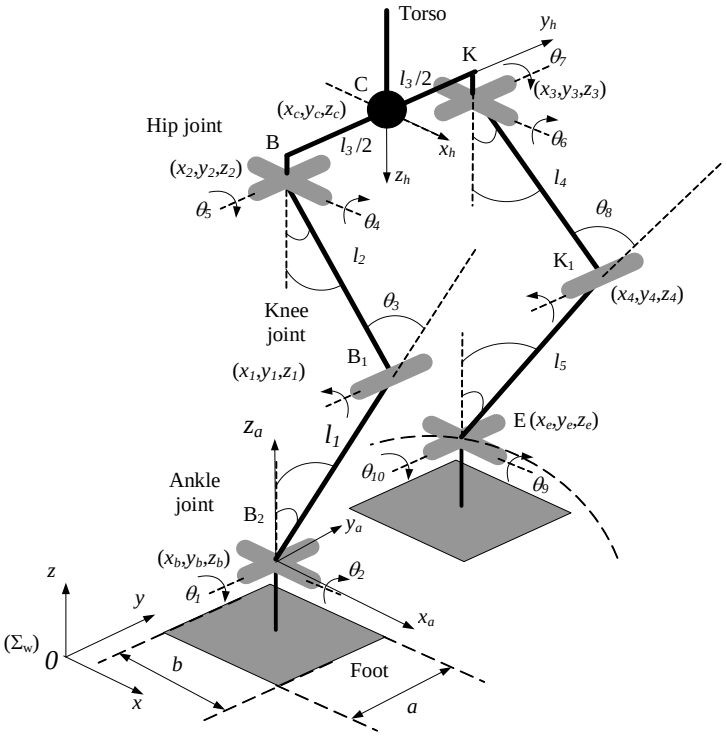

Fig. 1: Configuration of 10 DOF biped robot model.

The biped robot consists of five links that are one torso, two links in each leg with upper link and lower link, and two feet. The two legs of the biped robot are connected with torso via two DOF rotating hip joints. Hip joints can rotate the legs in the angles θ_5 for left leg and θ_7 for right leg on sagittal plane, and in the angles θ_4 for left leg and θ_6 for right leg on frontal plane. The upper links are connected with the lower links via one DOF rotating knee joints which can rotate only on sagittal plane. Right knee joint can rotate lower link and upper link of the right leg in angle θ_3, and left knee joint can rotate lower link and upper link of the left leg in angle θ_8. The lower links are connected with feet via two DOF ankle joints. The ankle joints can rotate the feet in angle θ_1 (for left leg) and θ_{10} (for right leg) on the sigattal plane, and in angle θ_2 for left leg and θ_9 for right leg on the in frontal plane. All the rotating joints are considered to be friction free and each one is driven by one DC motor.

In choosing Cartesian coordinate Σ_a whose origin is taken on the ankle joint, position of the center of the pelvis link is expressed as follows:

$$x_{ca} = l_1 \sin\theta_1 - l_2 \sin(\theta_3 - \theta_1) \quad (1)$$

$$y_{ca} = l_1 \sin\theta_2 + l_2 \cos(\theta_3 - \theta_1)\sin\theta_2 + \frac{l_3}{2}\cos(\theta_2 + \theta_4) \quad (2)$$

$$z_{ca} = l_1 \cos\theta_1 \cos\theta_2 + l_2 \cos(\theta_3 - \theta_1)\cos\theta_2 - \frac{l_3}{2}\sin(\theta_2 + \theta_4) \quad (3)$$

where x_{ca}, y_{ca} and z_{ca} are position of the center of the pelvis link in the coordinate system Σ_a.
Similarly, position of the ankle joint of swinging leg is expressed in the coordinate system Σ_h as:

$$x_{eh} = l_4 \sin\theta_7 - l_5 \sin(\theta_8 - \theta_7) \quad (4)$$

$$y_{eh} = \frac{l_3}{2} + l_4 \sin\theta_6 - l_5 \cos(\theta_8 - \theta_7)\sin\theta_6 \quad (5)$$

$$z_{eh} = l_4 \cos\theta_6 \cos\theta_7 + l_5 \cos(\theta_8 - \theta_7)\cos\theta_6 \quad (6)$$

It is assumed that the center of mass of each link is concentrated at the tip of the link.
The center of mass of the robot can be obtained as follows:

$$x_{com} = \frac{m_b x_b + m_1 x_1 + m_2 x_2 + m_c x_c + m_3 x_3 + m_4 x_4 + m_e x_e}{m_b + m_1 + m_2 + m_c + m_3 + m_4 + m_e} \quad (7)$$

$$y_{com} = \frac{m_b y_b + m_1 y_1 + m_2 y_2 + m_c y_c + m_3 y_3 + m_4 y_4 + m_e y_e}{m_b + m_1 + m_2 + m_c + m_3 + m_4 + m_e} \quad (8)$$

$$z_{com} = \frac{m_b z_b + m_1 z_1 + m_2 z_2 + m_c z_c + m_3 z_3 + m_4 z_4 + m_e z_e}{m_b + m_1 + m_2 + m_c + m_3 + m_4 + m_e} \quad (9)$$

where
m_b, m_1, m_2, m_c, m_3, m_4 and m_e are mass of the ankle joint of the right leg B_2, knee joint of the right leg B_1, hip joint of the right leg B, center of the pelvis link C, hip joint of the left leg K, knee joint of the left leg K_1 and ankle joint of the left leg E.
(x_b, y_b, z_b), (x_e, y_e, z_e), (x_1, y_1, z_1), (x_4, y_4, z_4), (x_2, y_2, z_2), (x_3, y_3, z_3) and (x_c, y_c, z_c) are coordinates of the ankle joints B_2, E, knee joints B_1, K_1, hip joints B, K, and center of pelvis link C.
It is assumed that the mass of links of legs is negligible compared with mass of the trunk. Eqs. (7)~(9) can be rewritten as follows:

$$x_{com} = x_c, \; y_{com} = y_c \text{ and } z_{com} = z_c \quad (10)$$

This means that the center of mass (COM) is concentrated at the center of the pelvis link.

2.2 Dynamic Model of Biped Robot

When the biped robot is supported by one leg, the dynamics of the robot can be approximated by a simple 3D inverted pendulum whose base is the foot of biped robot and head is COM of biped robot as shown in Fig. 2. The length of inverted pendulum r is able to be expanded or contracted. The position of the COM of the inverted pendulum C(x_{ca}, y_{ca}, z_{ca}) in the Cartesian coordinate can be uniquely specified by $\boldsymbol{q} = [\theta_r, \theta_p, r]^T$ in the polar coordinate as follows [1]:

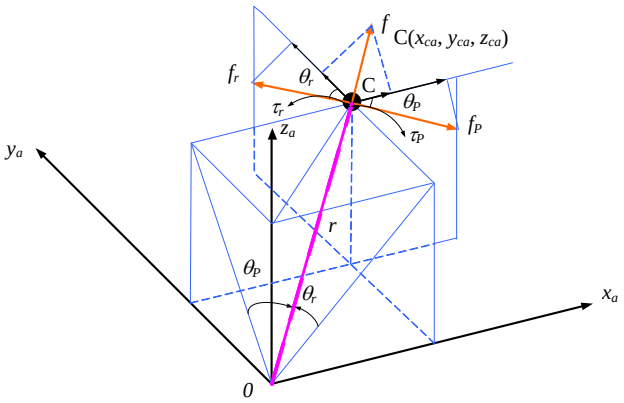

Fig. 2: Three dimension (3D) inverted pendulum.

$$x_{ca} = r\sin\theta_p \equiv rS_p \quad (11)$$

$$y_{ca} = -r\sin\theta_r \equiv -rS_r \quad (12)$$

$$z_{ca} = r\sqrt{1 - \sin^2\theta_r - \sin^2\theta_p} \equiv rD \quad (13)$$

where $S_r \equiv \sin\theta_r$, $S_p \equiv \sin\theta_p$, $C_p \equiv \cos\theta_p$, $C_r \equiv \cos\theta_r$, and $D \equiv \sqrt{1 - \sin^2\theta_p - \sin^2\theta_r}$.
$[\tau_r, \tau_p, f]^T$ are defined as the actuator torques and force associated with the variables $[\theta_r, \theta_p, r]^T$. The Lagrangian of the 3D inverted pendulum is

$$L = \frac{1}{2} m(\dot{x}_{ca}^2 + \dot{y}_{ca}^2 + \dot{z}_{ca}^2) - mgz_{ca} \quad (14)$$

where m is the total mass of the biped robot, and g is the gravitational acceleration.
Based on the Largange's equation, the dynamics of 3D inverted pendulum can be obtained in the Cartesian coordinate as follows:

$$m\begin{bmatrix} \ddot{x}_{ca} \\ \ddot{y}_{ca} \\ \ddot{z}_{ca} \end{bmatrix} = \left(\boldsymbol{J}^T\right)^{-1} \begin{bmatrix} \tau_r \\ \tau_p \\ f \end{bmatrix} + \begin{bmatrix} 0 \\ 0 \\ -mg \end{bmatrix}. \quad (15)$$

where $\boldsymbol{J}$ is Jacobian matrix which is expressed as

$$\boldsymbol{J} = \frac{\partial \boldsymbol{p}}{\partial \boldsymbol{q}} = \begin{bmatrix} 0 & rC_p & S_p \\ -rC_r & 0 & -S_r \\ -\frac{rC_rS_r}{D} & -\frac{rC_pS_p}{D} & D \end{bmatrix}. \quad (16)$$

The dynamics equation of inverted pendulum along y_a axis can be obtained as

$$m\left(-z_{ca}\ddot{y}_{ca} + y_{ca}\ddot{z}_{ca}\right) = \tau_x - mgy_{ca}. \quad (17)$$

where $\tau_x \equiv \frac{D}{C_r}\tau_r$ is the torque around x_a axis.

Using similar procedure, the dynamics equation of inverted pendulum along x_a axis can be derived as

$$m\left(z_{ca}\ddot{x}_{ca} - x_{ca}\ddot{z}_{ca}\right) = \tau_y + mgx_{ca} \quad (18)$$

where $\tau_y \equiv \frac{D}{C_p}\tau_p$ is the torque around y_a axis.

There are many classes of moving pattern of inverted pendulum. For selecting one of them, a constraint is applied to limit the motion of the inverted pendulum. That is, the motions of the COM of inverted pendulum are constrained on the plane whose normal vector $\boldsymbol{v_{cp}}$ is $[k_x,k_y,-1]^T$ and z_a intersection is z_{cd} as shown in Fig. 3.

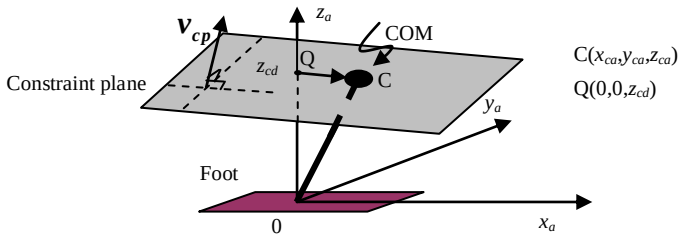

Fig. 3: Motion of inverted pendulum on constraint plane.

It is assumed that the constraint plane intersects the z_a axis at $Q(0,0,z_{cd})$ as shown in Fig. 3. Because $C(x_{ca},y_{ca},z_{ca})$ is located on the constraint plane, vector $\boldsymbol{v_{cp}}$ is perpendicular to vector $\overrightarrow{QC}$. The constraint condition of the motion of the COM of inverted pendulum is expressed as

$$z_{ca} = k_x x_{ca} + k_y y_{ca} + z_{cd} \quad (19)$$

where k_x, k_y and z_{cd} are constants.
When the biped robot walks on a rugged terrain, the normal vector of the constraint plane should be perpendicular to the slope of the ground, and z_a intersection z_{cd} in the coordinate system Σ_a is set as distance between COM and the ground.
The second order derivative of Eq. (19) is

$$\ddot{z}_{ca} = k_x \ddot{x}_{ca} + k_y \ddot{y}_{ca}. \quad (20)$$

Substituting Eqs. (19)~(20) into Eqs. (17)~(18), the equation of motion of 3D inverted pendulum under constraint can be expressed as

$$\ddot{y}_{ca} = \frac{g}{z_{cd}} y_{ca} - \frac{k_x}{z_{cd}}\left(x_{ca}\ddot{y}_{ca} - \ddot{x}_{ca}y_{ca}\right) - \frac{1}{mz_{cd}}\tau_x \quad (21)$$

$$\ddot{x}_{ca} = \frac{g}{z_{cd}} x_{ca} + \frac{k_y}{z_{cd}}\left(x_{ca}\ddot{y}_{ca} - \ddot{x}_{ca}y_{ca}\right) + \frac{1}{mz_{cd}}\tau_y. \quad (22)$$

It is assumed that the biped robot walks on the flat floor and horizontal plane. In this case, k_x and k_y are set to

zero. It means that the COM of inverted pendulum moves on a horizontal plane which has height $z_{ca} = z_{cd}$ as shown in Fig. 3.
Eqs. (21)~(22) can be rewritten as:

$$\ddot{y}_{ca} = \frac{g}{z_{cd}} y_{ca} - \frac{1}{mz_{cd}} \tau_x \quad (23)$$

$$\ddot{x}_{ca} = \frac{g}{z_{cd}} x_{ca} + \frac{1}{mz_{cd}} \tau_y . \quad (24)$$

When the inverted pendulum moves on the horizontal plane, the dynamic equations along the x_a axis and y_a axis are independent each other and can be rewritten as linear differential equations.
(x_{zmp}, y_{zmp}) is defined as location of ZMP on the floor as shown in Fig. 4.

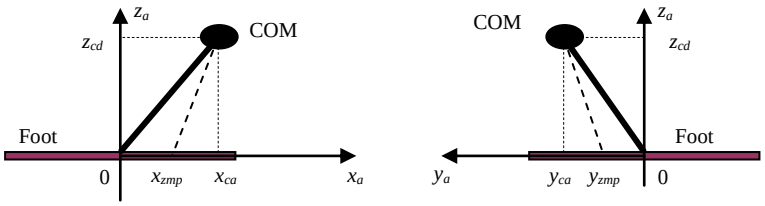

Fig. 4: ZMP of inverted pendulum.

(x_{ca}, y_{ca}, z_{ca}) is projection of COM in the coordinate system Σ_a.
ZMP is a point where the net support torques from floor about x_a axis and y_a axis are zero. From D'Alembert's principle, ZMP of inverted pendulum under constraint can be expressed as

$$x_{zmp} = x_{ca} - \frac{z_{cd}}{g} \ddot{x}_{ca} \quad (25)$$

$$y_{zmp} = y_{ca} - \frac{z_{cd}}{g} \ddot{y}_{ca} . \quad (26)$$

Eq. (25) shows that position of ZMP along x_a axis depends only on the position and acceleration of COM along x_a axis. Similarly, position of ZMP along y_a axis does not depend on the position of COM along x_a axis, but it depends only on the position and acceleration of COM along y_a axis.
When the biped robot moves with slow speed, Eqs. (25)~(26) can be approximated as Eqs. (27). It is shown that coordinate of the ZMP is projection of COM.

$$x_{zmp} = x_{ca} \text{ and } y_{zmp} = y_{ca} \quad (27)$$

Since there are no actions torques that cause robot to fall down at ZMP, ZMP is very important for walking robot and generally used as dynamic criterion for gait planning and control. During the walking of robot, ZMP is located inside of the footprint of supported foot or inside the supported polygon.

III. WALKING PATTERN GENERATION

The objective of controlling the biped robot is to realize a stable walking or running. The stable walking or running of the biped robot depends on walking pattern. Walking pattern generation is used to generate a trajectory for COM of the biped robot. For the stable walking or running of the biped robot, the walking pattern should satisfy the condition that the ZMP of the biped robot always exists inside the stable region. Since position of COM of the biped robot has the close relationship with position of ZMP as shown in Eqs. (25)~(26), trajectory of COM can be obtained from the trajectory of ZMP. Based on a sequence of desired footprint and period time of each step of the biped robot, a reference trajectory of ZMP can be specified. Fig. 5 illustrates footprint and reference trajectory of ZMP to guarantee stable gait.

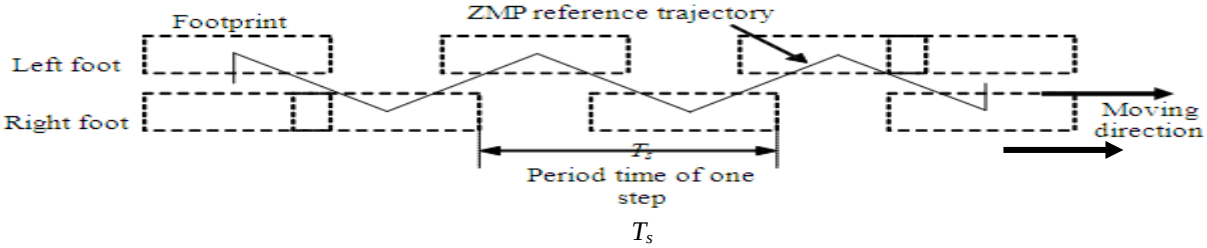

Fig. 5: Footprint and reference trajectory of ZMP.

3.1 Walking Pattern Generation Based on Servo Control of ZMP

When a biped robot is modeled as 3D inverted pendulum which is moved on horizontal plane, the ZMP's position of the biped robot is expressed by linear independent equations along x_a and y_a directions which are shown as Eqs. (25)~(26).

$u_x = \frac{d}{dt}\ddot{x}_{ca} = \dddot{x}_{ca}$ and $u_y = \frac{d}{dt}\ddot{y}_{ca} = \dddot{y}_{ca}$ are defined as the time derivative of the horizontal acceleration along x_a and y_a directions of the COM, u_x and u_y are introduced as inputs. Eqs. (25)~(26) can be rewritten in strictly proper form as follows:

$$\underbrace{\begin{bmatrix}\dot{x}_{ca}\\ \ddot{x}_{ca}\\ \dddot{x}_{ca}\end{bmatrix}}_{\dot{x}_x(t)} = \underbrace{\begin{bmatrix}0 & 1 & 0\\ 0 & 0 & 1\\ 0 & 0 & 0\end{bmatrix}}_{A}\underbrace{\begin{bmatrix}x_{ca}\\ \dot{x}_{ca}\\ \ddot{x}_{ca}\end{bmatrix}}_{x_x(t)} + \underbrace{\begin{bmatrix}0\\ 0\\ 1\end{bmatrix}}_{B}u_x, \quad (28)$$

$$x_{zmp} = \underbrace{\begin{bmatrix}1 & 0 & -\frac{z_{cd}}{g}\end{bmatrix}}_{C}\underbrace{\begin{bmatrix}x_{ca}\\ \dot{x}_{ca}\\ \ddot{x}_{ca}\end{bmatrix}}_{x_x(t)},$$

$$\underbrace{\begin{bmatrix}\dot{y}_{ca}\\ \ddot{y}_{ca}\\ \dddot{y}_{ca}\end{bmatrix}}_{\dot{x}_y(t)} = \underbrace{\begin{bmatrix}0 & 1 & 0\\ 0 & 0 & 1\\ 0 & 0 & 0\end{bmatrix}}_{A}\underbrace{\begin{bmatrix}y_{ca}\\ \dot{y}_{ca}\\ \ddot{y}_{ca}\end{bmatrix}}_{x_y(t)} + \underbrace{\begin{bmatrix}0\\ 0\\ 1\end{bmatrix}}_{B}u_y, \quad (29)$$

$$y_{zmp} = \underbrace{\begin{bmatrix}1 & 0 & -\frac{z_{cd}}{g}\end{bmatrix}}_{C}\underbrace{\begin{bmatrix}y_{ca}\\ \dot{y}_{ca}\\ \ddot{y}_{ca}\end{bmatrix}}_{x_y(t)}.$$

where position of ZMP along x_a axis, x_{zmp}, is output of system (28), position of ZMP along y_a axis, y_{zmp}, is output of system (29), x_{ca} and y_{ca} are position of COM with respect to x_a and y_a axes, and $\dot{x}_{ca}$, $\ddot{x}_{ca}$, $\dot{y}_{ca}$, $\ddot{y}_{ca}$ are horizontal velocity and acceleration with respect to x_a and y_a directions, respectively.

Instead of solving differential Eqs. (25)~(26), position of COM can be obtained by constructing a controller to track the ZMP as output of Eqs. (28)~(29). When x_{zmp} and y_{zmp} are controlled to track reference trajectory of ZMP, COM trajectory can be obtained from state variables x_{ca} and y_{ca}. According to this pattern, the walking or running of the biped robot are stable.

By constructing ZMP tracking control systems, walking pattern generation problem turns into designing tracking controller to track ZMP's reference trajectory.

To control output of the systems with Eqs. (28)~(29), There are many type of controllers can be applied. In this paper, a discrete time optimal control theory is chosen to design tracking controller.

The systems (28) and (29) can be discretized with sampling time T as follows [6]:

$$\boldsymbol{x}_x[(k+1)] = \boldsymbol{\Phi}(T)\boldsymbol{x}_x(k) + \boldsymbol{\theta}(T)u_x(k) \quad (30)$$
$$x_{zmp}(k) = \boldsymbol{C}\boldsymbol{x}_x(k)$$
$$\boldsymbol{x}_y[(k+1)] = \boldsymbol{\Phi}(T)\boldsymbol{x}_y(k) + \boldsymbol{\theta}(T)u_y(k) \quad (31)$$
$$y_{zmp}(k) = \boldsymbol{C}\boldsymbol{x}_y(k)$$

where $\boldsymbol{x}_x(k) \equiv [x(kT) \quad \dot{x}(kT) \quad \ddot{x}(kT)]^T$ and $\boldsymbol{x}_y(k) \equiv [y(kT) \quad \dot{y}(kT) \quad \ddot{y}(kT)]^T$ are states vectors, $u_x(k) \equiv u_x(kT)$ and $u_y(k) \equiv u_y(kT)$ are input signals, and $x_{zmp}(k) \equiv x_{zmp}(kT)$ and $y_{zmp}(k) \equiv y_{zmp}(kT)$ are outputs, $\boldsymbol{\Phi}(T) = \begin{bmatrix}1 & T & T^2/2\\ 0 & 1 & T\\ 0 & 0 & 1\end{bmatrix}$ and $\boldsymbol{\theta}(T) = \begin{bmatrix}T^3/6\\ T^2/2\\ T\end{bmatrix}$.

The controllability matrix of systems (30) and (31) has full rank. The system is controllable and stabilizable [6]. Similarly, observability matrix $\boldsymbol{O}_d$ of them has full rank.

3.2 Controller Design for ZMP Tracking Control

In this section, discrete time optimal tracking controller utilizing the future values of reference input is designed to control the systems (30) and (31) to track ZMP reference input.

A time invariant discrete time system is considered as follows:

$$\begin{aligned} \boldsymbol{x}[(k+1)] &= \boldsymbol{A}_d \boldsymbol{x}(k) + \boldsymbol{B}_d u(k) \\ y(k) &= \boldsymbol{C}_d \boldsymbol{x}(k) \end{aligned} \quad (32)$$

where $\boldsymbol{x}(k) \in \Re^{n\times 1}$ is $n\times 1$ state vector, $y(k) \in \Re$ is output, $u(k) \in \Re$ is control input, and $\boldsymbol{A}_d \in \Re^{n\times n}$, $\boldsymbol{B}_d \in \Re^{n\times 1}$, $\boldsymbol{C}_d \in \Re^{1\times n}$ are matrices with corresponding dimensions.

An error signal $e(k) \in \Re$ is defined as the difference between reference input $r(k)$ and output of the system $y(k)$ as follows:

$$e(k) = r(k) - y(k) \quad (33)$$

It is denoted that the incremental control input is $\Delta u(k) = u(k) - u(k-1)$ and the incremental state is $\Delta \boldsymbol{x}(k) = \boldsymbol{x}(k) - \boldsymbol{x}(k-1)$. If the system (32) is controllable and observable, it can be rewritten in the increment as follows:

$$\begin{aligned} \Delta \boldsymbol{x}[(k+1)] &= \boldsymbol{A}_d \Delta \boldsymbol{x}(k) + \boldsymbol{B}_d \Delta u(k) \\ y(k) &= \boldsymbol{C}_d \boldsymbol{x}(k) \end{aligned} \quad (34)$$

The error at the $k+1^{th}$ sample time can be obtained from Eq. (33) as

$$e(k+1) = r(k+1) - y(k+1). \quad (35)$$

Substituting Eq. (34) into result of subtracting Eq. (33) from Eq. (35) yields

$$e(k+1) = e(k) + \Delta r(k+1) - \boldsymbol{C}_d \boldsymbol{A}_d \Delta \boldsymbol{x}(k) - \boldsymbol{C}_d \boldsymbol{B}_d \Delta u(k). \quad (36)$$

where $\Delta r(k+1) = r(k+1) - r(k) \in \Re$

From the first row of Eq. (34) and Eq. (36), the error system can be obtained as

$$\underbrace{\begin{bmatrix} e(k+1) \\ \Delta \boldsymbol{x}(k+1) \end{bmatrix}}_{\boldsymbol{X}(k+1)} = \underbrace{\begin{bmatrix} 1 & -\boldsymbol{C}_d \boldsymbol{A}_d \\ \boldsymbol{0}_{n\times 1} & \boldsymbol{A}_d \end{bmatrix}}_{\boldsymbol{A}_E} \underbrace{\begin{bmatrix} e(k) \\ \Delta \boldsymbol{x}(k) \end{bmatrix}}_{\boldsymbol{X}(k)} + \underbrace{\begin{bmatrix} 1 \\ \boldsymbol{0}_{n\times 1} \end{bmatrix}}_{\boldsymbol{G}_R} \Delta r(k+1) + \underbrace{\begin{bmatrix} -\boldsymbol{C}_d \boldsymbol{B}_d \\ \boldsymbol{B}_d \end{bmatrix}}_{\boldsymbol{G}} \Delta u(k) \quad (37)$$

where $\boldsymbol{X}(k) \in \Re^{(1+n)\times 1}$, $\boldsymbol{A}_E \in \Re^{(1+n)\times(1+n)}$, $\boldsymbol{G}_R \in \Re^{(1+n)\times 1}$ and $\boldsymbol{G} \in \Re^{(1+n)\times 1}$.

It is assumed that at each time k, the reference inputs of the error system (37) can be known for N future values as well as the present and the past values are available.

A scalar cost function of the quadratic form is chosen as

$$J = \sum_{k=0}^{\infty} \left[\boldsymbol{X}^T(k) \boldsymbol{Q} \boldsymbol{X}(k) + R \Delta u^2(k) \right] \quad (38)$$

where $\boldsymbol{Q} = \begin{bmatrix} Q_e & \boldsymbol{0}_{1\times n} \\ \boldsymbol{0}_{n\times 1} & \boldsymbol{0}_{n\times n} \end{bmatrix} \in \Re^{(1+n)\times(1+n)}$ is semi-positive definite matrix, $Q_e \in \Re$, and $R \in \Re$ are positive scalar.

An optimal problem is solved by minimizing the cost function (38).

It is assumed that N future values of the reference input $r(k+1), r(k+2), \cdots, r(k+N)$ can be utilized. The future values of reference beyond time $(k+N)$ are approximated by $r(k+N)$. It means that the following is satisfied.

$$\Delta r(k+i) = 0 \qquad (i = N+1, N+2, \ldots). \quad (39)$$

$\boldsymbol{X}_R(k) = \left[\Delta r(k+1) \quad \Delta r(k+2) \quad \cdots \quad \Delta r(k+N) \right]^T \in \Re^{N\times 1}$ is defined as a future reference input incremental vector depending on N incremental future values of the reference input.

The augmented error system with future values of reference input is obtained as

$$\begin{bmatrix} \boldsymbol{X}(k+1) \\ \boldsymbol{X}_R(k+1) \end{bmatrix} = \begin{bmatrix} \boldsymbol{A}_E & \boldsymbol{G}_{PR} \\ \boldsymbol{0}_{N\times(n+1)} & \boldsymbol{A}_R \end{bmatrix} \begin{bmatrix} \boldsymbol{X}(k) \\ \boldsymbol{X}_R(k) \end{bmatrix} + \begin{bmatrix} \boldsymbol{G} \\ \boldsymbol{0}_{(Nm)\times r} \end{bmatrix} \Delta \boldsymbol{u}(k). \quad (40)$$

where $\boldsymbol{G}_{PR} = \begin{bmatrix} \boldsymbol{G}_R & \boldsymbol{0}_{(1+n)\times 1} & \cdots & \boldsymbol{0}_{(1+n)\times 1} \end{bmatrix} \in \Re^{(1+n)\times N}$, and $\boldsymbol{A}_R = \begin{bmatrix} 0 & 1 & 0 & \cdots & 0 \\ \vdots & & \ddots & \ddots & \vdots \\ \vdots & & & \ddots & 0 \\ \vdots & & & & 1 \\ 0 & \cdots & \cdots & \cdots & 0 \end{bmatrix} \in \Re^{N\times N}$

The cost function (38) can be rewritten as

$$J=\sum_{k=0}^{\infty}\left\{\begin{bmatrix}\boldsymbol{X}^T(k) & \boldsymbol{X}_R^T(k)\end{bmatrix}\begin{bmatrix}\boldsymbol{Q} & \boldsymbol{0}_{(n+1)\times N}\\ \boldsymbol{0}_{N\times(n+1)} & \boldsymbol{0}_{N\times N}\end{bmatrix}\begin{bmatrix}\boldsymbol{X}(k)\\ \boldsymbol{X}_R(k)\end{bmatrix}+R\Delta u^2(k)\right\} \quad (41)$$

The optimal control signal $\Delta u(k)$ that minimizes cost function (41) of system (40) can be obtained as [6]

$$\Delta u(k)=-\left[\boldsymbol{R}+\begin{bmatrix}\boldsymbol{G}^T & \boldsymbol{0}_{N\times 1}\end{bmatrix}\boldsymbol{P}\begin{bmatrix}\boldsymbol{G}\\ \boldsymbol{0}_{N\times 1}\end{bmatrix}\right]^{-1}\begin{bmatrix}\boldsymbol{G}^T & \boldsymbol{0}_{N\times 1}\end{bmatrix}\boldsymbol{P}\begin{bmatrix}\boldsymbol{A}_E & \boldsymbol{G}_{PR}\\ \boldsymbol{0}_{N\times(n+1)} & \boldsymbol{A}_R\end{bmatrix}\begin{bmatrix}\boldsymbol{X}(k)\\ \boldsymbol{X}_R(k)\end{bmatrix} \quad (42)$$

where $\boldsymbol{P}$ is semi-positive definite matrix that is a solution of the algebraic Ricatti equation corresponding to Eq. (40) [6].

$\boldsymbol{P}$ can be partitioned as follows:

$$\boldsymbol{P}=\begin{bmatrix}\boldsymbol{P}_1 & \boldsymbol{W}\\ \boldsymbol{W}^T & \boldsymbol{P}_2\end{bmatrix}\in\Re^{(1+n+N)\times(1+n+N)}. \quad (43)$$

where $\boldsymbol{P}_1\in\Re^{(n+1)\times(n+1)}$, $\boldsymbol{P}_2\in\Re^{N\times N}$ and $\boldsymbol{W}\in\Re^{(n+1)\times N}$

$$\boldsymbol{P}_1=\boldsymbol{Q}+\boldsymbol{A}_E^T\boldsymbol{P}_1\boldsymbol{A}_E-\boldsymbol{A}_E^T\boldsymbol{P}_1\boldsymbol{G}\left[\boldsymbol{R}+\boldsymbol{G}^T\boldsymbol{P}_1\boldsymbol{G}\right]^{-1}\boldsymbol{G}^T\boldsymbol{P}_1\boldsymbol{A}_E \quad (44)$$

$$\boldsymbol{W}=\boldsymbol{A}_E^T\left(\boldsymbol{I}-\boldsymbol{P}_1\boldsymbol{G}\left(\boldsymbol{R}+\boldsymbol{G}^T\boldsymbol{P}_1\boldsymbol{G}\right)^{-1}\boldsymbol{G}^T\right)\left(\boldsymbol{P}_1\boldsymbol{G}_{PR}+\boldsymbol{W}\boldsymbol{A}_R\right) \quad (45)$$

The optimal control signal $\Delta u(k)$ becomes

$$\Delta u(k)=\begin{bmatrix}\boldsymbol{K}_1 & \boldsymbol{K}_2\end{bmatrix}\begin{bmatrix}\boldsymbol{X}(k)\\ \boldsymbol{X}_R(k)\end{bmatrix}=\boldsymbol{K}_1\boldsymbol{X}(k)+\boldsymbol{K}_2\boldsymbol{X}_R(k) \quad (45)$$

Where $\boldsymbol{K}_1=\begin{bmatrix}\boldsymbol{K}_{1e} & \boldsymbol{K}_{1x}\end{bmatrix}=-\left[\boldsymbol{R}+\boldsymbol{G}^T\boldsymbol{P}_1\boldsymbol{G}\right]^{-1}\boldsymbol{G}^T\boldsymbol{P}_1\boldsymbol{A}_E\in\Re^{1\times(1+n)}$ is defined as feedback gain matrix and $\boldsymbol{K}_2=-\left[\boldsymbol{R}+\boldsymbol{G}^T\boldsymbol{P}_1\boldsymbol{G}\right]^{-1}\boldsymbol{G}^T\left(\boldsymbol{P}_1\boldsymbol{G}_{PR}+\boldsymbol{W}\boldsymbol{A}_R\right)\in\Re^{1\times N}$ is defined as feed forward matrix.

Corresponding with *N* future values of reference input, feed forward matrix $\boldsymbol{K}_2$ and $\boldsymbol{W}$ can be rewritten as

$$\boldsymbol{W}=\begin{bmatrix}\boldsymbol{W}(1) & \boldsymbol{W}(2) & \cdots & \boldsymbol{W}(N)\end{bmatrix} \quad (47)$$

$$\boldsymbol{K}_2=\begin{bmatrix}\boldsymbol{K}_2(1) & \boldsymbol{K}_2(2) & \cdots & \boldsymbol{K}_2(N)\end{bmatrix} \quad (48)$$

where $\boldsymbol{W}(i)\in\Re^{(n+1)\times 1}, i=1,2\ldots,N$; $\boldsymbol{K}_2(i)\in\Re, i=1,2\ldots,N$

Using Eq. (40) and Eq. (47), Eq. (48) is re-expressed as

$$\boldsymbol{K}_2=-\left[\boldsymbol{R}+\boldsymbol{G}^T\boldsymbol{P}_1\boldsymbol{G}\right]^{-1}\boldsymbol{G}^T\times\left\{\boldsymbol{P}_1\begin{bmatrix}\boldsymbol{G}_R & \boldsymbol{0}_{(n+1)\times 1} & \cdots & \boldsymbol{0}_{(n+1)\times 1}\end{bmatrix}+\begin{bmatrix}\boldsymbol{0} & \boldsymbol{W}(1) & \cdots & \boldsymbol{W}(N-1)\end{bmatrix}\right\} \quad (49)$$

From Eq. (40) and Eq. (47), Eq. (44) becomes

$$\begin{bmatrix}\boldsymbol{W}(1) & \boldsymbol{W}(2) & \cdots & \boldsymbol{W}(N)\end{bmatrix}=\boldsymbol{A}_E^T\left[\boldsymbol{I}-\boldsymbol{P}_1\boldsymbol{G}\left(\boldsymbol{R}+\boldsymbol{G}^T\boldsymbol{P}_1\boldsymbol{G}\right)^{-1}\boldsymbol{G}^T\right]\times\left\{\boldsymbol{P}_1\begin{bmatrix}\boldsymbol{G}_R & \boldsymbol{0}_{(n+1)\times 1} & \cdots & \boldsymbol{0}_{(n+1)\times 1}\end{bmatrix}+\begin{bmatrix}\boldsymbol{0}_{(n+1)\times 1} & \boldsymbol{W}(1) & \cdots & \boldsymbol{W}(N-1)\end{bmatrix}\right\} \quad (50)$$

It is defined that $\boldsymbol{F}=\boldsymbol{A}_E^T\left(\boldsymbol{I}-\boldsymbol{P}_1\boldsymbol{G}\left(\boldsymbol{R}+\boldsymbol{G}^T\boldsymbol{P}_1\boldsymbol{G}\right)^{-1}\boldsymbol{G}^T\right)$.

Eq. (50) yields

$$\boldsymbol{W}(i)=\boldsymbol{F}^i\boldsymbol{P}_1\boldsymbol{G}_R \qquad i=1,2,..,N \quad (51)$$

From Eq. (49), $\boldsymbol{K}_2(i),\ i=1,2,\ldots,N$, can be obtained as

$$\boldsymbol{K}_2(i)=-\left[\boldsymbol{R}+\boldsymbol{G}^T\boldsymbol{P}_1\boldsymbol{G}\right]^{-1}\boldsymbol{G}^T\boldsymbol{F}^{i-1}\boldsymbol{P}_1\boldsymbol{G}_R. \quad (52)$$

Eq. (45) can be rewritten as

$$\Delta u(k)=K_{1e}e(k)+\boldsymbol{K}_{1x}\Delta\boldsymbol{x}(k)+\sum_{i=1}^{N}K_2(i)\Delta r(k+i) \quad (53)$$

By taking the initial values as zero and integrating both side of Eq. (53), the control law $u(k)$ can be obtained as

$$u(k)=K_{1e}\frac{z}{z-1}e(k)+\boldsymbol{K}_{1x}\boldsymbol{x}(k)+\sum_{i=1}^{N}K_2(i)\,r(k+i) \quad (54)$$

The block diagram of the closed loop ZMP tracking control system using discrete time optimal tracking controller utilizing the future values of reference input is shown in Fig. 6.

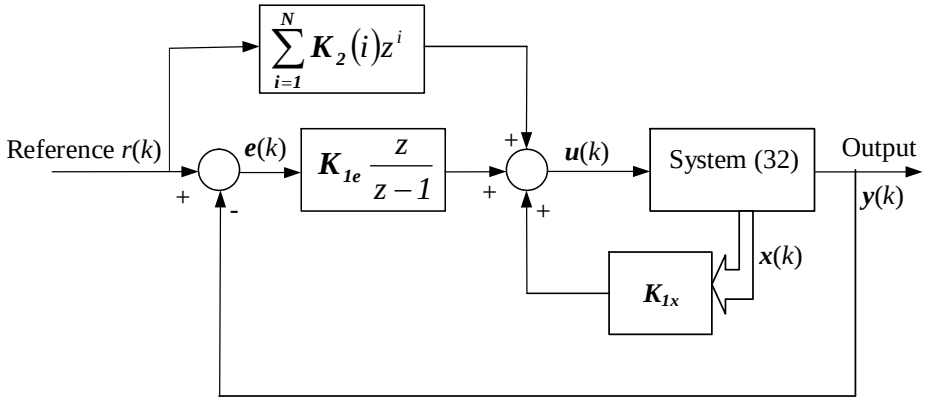

Fig. 6: Closed loop ZMP control system with discrete time optimal tracking controller.

IV. WALKING CONTROL OF THE BIPED ROBOT

Based on the walking pattern generation discussed in previous sections, a trajectory of COM of the biped robot is generated by ZMP servo control system. The ZMP reference input trajectory of the ZMP servo system is chosen to satisfy the stable condition of the biped robot. The control objective for the stable walking of the biped robot is to track the center of pelvis link to the COM trajectory. The inverse kinematics of the biped robot is solved to obtain the angle of each joint of the biped robot. The walking control of the biped robot is performed based on the solutions of the inverse kinematics which is solved by solid geometry method.

4.1 Inverse Kinematics of the Biped Robot

The configuration of a 10 DOF biped robot is shown in Fig. 1. The relationship between biped robot and 3D inverted pendulum is shown in Fig. 7. Solving the inverse kinematics problems directly from kinematics models is complex. An inverse kinematics based on the solid geometry method is presented in this section.

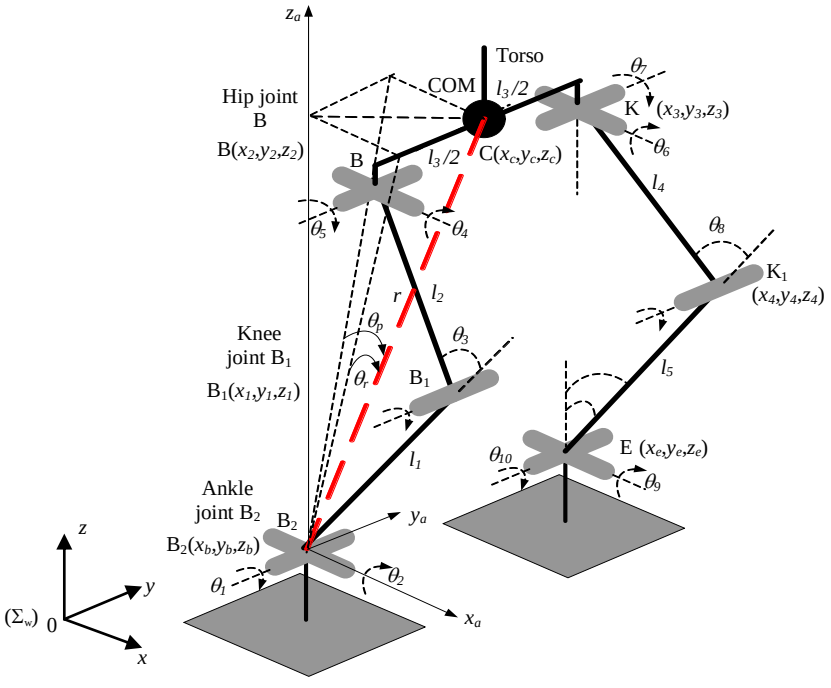

Fig. 7: Biped robot and 3D inverted pendulum.

During the walking of the biped robot, the following assumptions are supposed

- Trunk of robot is always located on the sagittal and lateral plane: when the trunk of robot is located on the sagittal and lateral plane, from the geometric structure of the biped robot, it is easy to obtain $\theta_2 = -\theta_4$ and $\theta_9 = -\theta_6$.

- The feet of robot are always parallel with floor: when the trunk of robot is on the sagittal plane, the feet of robot are parallel with floor if following conditions are satisfied

$$\theta_3 = \theta_1 + \theta_5, \quad \theta_8 = \theta_7 + \theta_{10}. \quad (55)$$

- The walking of the biped robot is divided into three phases: Two-legs supported, right-leg supported and left-leg supported. When the robot is supported by one leg, another leg swings.

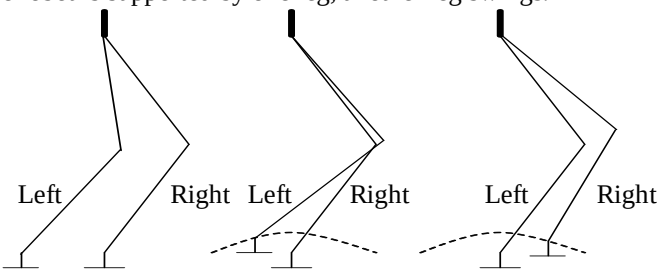

(a) Two-leg supported phase

(b) Right-leg supported and left-leg swinging phase

(c) Left-leg supported and right leg swinging phase

Fig. 8: Three walking phases of the biped robot.

- The origin of the 3D inverted pendulum is located at the center of the ankle joint of supported leg.

4.1.1 Inverse kinematics of biped robot in one-leg supported phase

It is supposed that biped robot is with the right-leg supported and left-leg swinging. The coordinate of the COM in coordinate system Σ_a whose origin is taken at the center of the ankle joint of supported leg can be obtained as

$$x_{ca} = x - x_b, \; y_{ca} = y - y_b \text{ and } z_{ca} = z - z_b \quad (56)$$

where (x,y,z) and (x_b,y_b,z_b) are coordinate of the COM and center of the ankle joint of supported leg in the world coordinate and (x_{ca},y_{ca},z_{ca}) is Coordinate of the COM in the coordinate Σ_a.
Solving Eqs. (11)~(13) at k^{th} sample time with $z_{ca} = z_{cd}$ yields

$$r(k) = \sqrt{z_{cd}^2(k) + x_{ca}^2(k) + y_{ca}^2(k)} \quad (57)$$

Since the trunk of robot is always located on the sagittal plane, the pelvis link is always on the horizontal plane $\square CBDC_1$ as shown in Fig. 9. The BC line is perpendicular to the line 0A at A, and it yields $\angle 0CB = \frac{\pi}{2} - \theta_r$.
Using the cosine's law, the length of 0B side of the triangle 0BC at the k^{th} sample time is obtained as follows:

$$h(k) = \sqrt{x_{ca}^2 + \left(y_{ca} - \frac{l_3}{2}\right)^2 + z_c^2} = \sqrt{\frac{l_3^2}{4} + r^2(k) - l_3 y_{ca}(k)} \quad (58)$$

The angle $\alpha(k)$ between l_2 and l_1 sides of the triangle $0BB_1$ is calculated by the cosine's law as follows:

$$\alpha(k) = \arccos\left(\frac{l_1^2 + l_2^2 - h^2(k)}{2 l_1 l_2}\right). \quad (59)$$

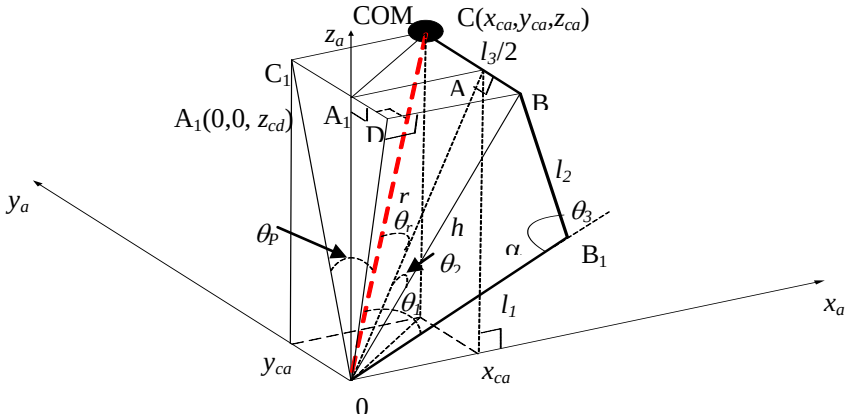

Fig. 9: Inverted pendulum and supported leg.

From $\alpha(k)$ in Eq. (59), the knee joint angle of the biped robot is gotten as Eq. (60).

$$\theta_3(k) = \pi - \alpha(k) \quad (60)$$

In Fig. 9, the BC line is perpendicular to the line 0A at A. From the right-triangle 0AB, the ankle joint angle $\theta_2(k)$ can be obtained as

$$\theta_2(k) = \angle \mathrm{A0B} = arcsin\left(\frac{y_{ca}(k) - \frac{l_3}{2}}{h(k)}\right). \quad (61)$$

Since height of COM of the biped robot is always kept equal to constant z_{cd} and COM is on sagittal plane during walking of biped robot, the BD line is perpendicular to $0y_a z_a$ plane. It means that the BD line is perpendicular to 0D line. The triangles OBB_1 and ODB lie on the same plane which contains the links l_1 and l_2 of the biped robot as shown in Fig. 9. The angle $\theta_1(k)$ can be obtained as follows

$$\theta_1(k) = \angle \mathrm{D0B} + \angle \mathrm{B0B}_1 = arcsin\left(\frac{x_{ca}(k)}{h(k)}\right) + arccos\left(\frac{h^2(k) + l_1^2 - l_2^2}{2h(k)l_1}\right). \quad (62)$$

4.1.2 Inverse kinematics of swinging leg

It is assumed that the biped robot is supported by right leg and is swung by left leg as shown in Fig. 10.

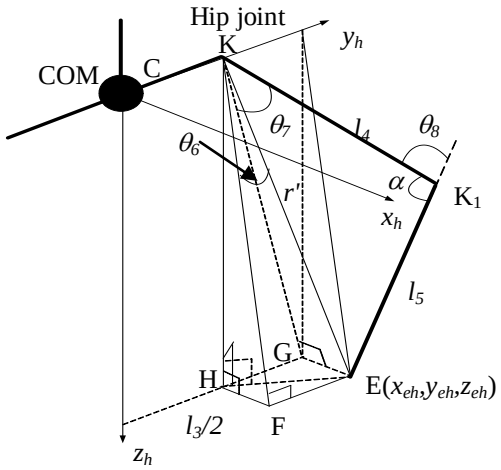

Fig. 10: Swinging leg of biped robot.

A coordinate system Σ_h with the origin taken at the middle of pelvis link is defined as shown in Fig. 10. During the swing of this leg, the coordinate y_{eh} of the foot of swinging leg is constant.

$r'(k)$ is defined as the distance between ankle joint and hip joint of swinging leg at the k^{th} sample time. It is expressed in the coordinate system Σ_h as follows:

$$r'(k)^2 = x_{eh}^2(k) + \left(y_{eh}(k) - \frac{l_3}{2}\right)^2 + z_{eh}^2(k) \quad (63)$$

where $(x_{eh}(k), y_{eh}(k), z_{eh}(k))$ is coordinate of the ankle joint of swinging leg in the coordinate Σ_h at the k^{th} sample time.

Since *EF* line is perpendicular to the line KF at F, the hip angle $\theta_6(k)$ of the swinging leg is obtained based on the right-triangle KEF as

$$\theta_6(k) = -arcsin\left(\frac{y_{eh}(k) - l_3/2}{r'(k)}\right) \quad (64)$$

The minus sign in (64) means counterclockwise.

The links l_4 and l_5 lie on the plane which contains right-triangle KGE. The hip angle $\theta_7(k)$ is equal to the angle between link l_4 and Cy_hz_h plane. It is can be expressed as

$$\theta_7(k) = \angle\text{GKE} + \angle\text{EKK}_1 = arcsin\left(\frac{x_{eh}(k)}{r'(k)}\right) + arccos\left(\frac{r'^2(k) + l_4^2 - l_5^2}{2r'(k)l_4}\right) \quad (65)$$

Using the cosine's law, the angle of knee of swinging leg can be obtained as

$$\theta_8(k) = \pi - \alpha_1 = \pi - arccos\left(\frac{l_5^2 + l_4^2 - r'^2(k)}{2l_5l_4}\right). \quad (66)$$

Similarly, when the biped robot is supported by left leg and is swung by right leg. The angles of right leg are calculated from Eqs. (64)~(66).

4.1.3 Inverse kinematics of biped robot in two-leg supported phase

It is assumed that the swinging leg of the biped robot contacts the ground after swinging phase as shown in Fig. 11. The biped robot is supported by two legs.

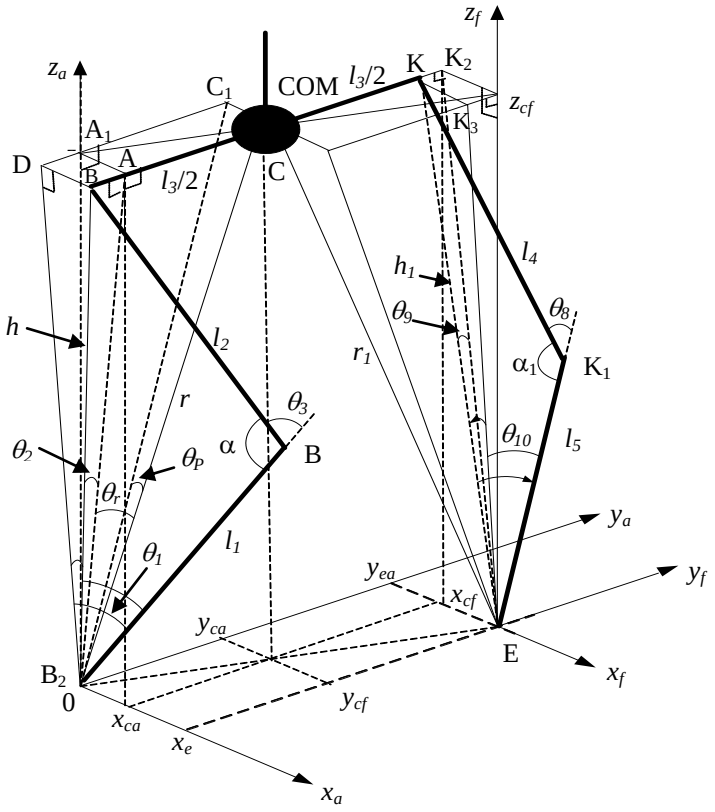

Fig. 11: Biped robot with two legs supported.

The coordinate of COM is expressed in coordinate system Σ_f whose origin is taken at the ankle joint of new supported leg as

$$x_{cf}(k) = x_{ca}(k) - x_{ea}(k) \quad (67)$$

$$y_{cf}(k) = y_{ca}(k) - y_{ea}(k) \quad (68)$$

$$z_{cf}(k) = z_{ca}(k) \quad (69)$$

where (x_{ea}, y_{ea}, z_{ea}) is coordinate of the ankle joint of the new supported leg in coordinate system Σ_a, (x_{ca}, y_{ca}, z_{ca}) is coordinate of the COM in coordinate system Σ_a and (x_{cf}, y_{cf}, z_{cf}) is coordinate of the COM in coordinate system Σ_f.

$r_1(k)$ is defined as distance between COM and ankle joint of the left leg. It is calculated based on the

coordinate of COM in coordinate system Σ_f as

$$r_1^2(k) = x_{cf}^2(k) + y_{cf}^2(k) + z_{cf}^2(k) \quad (70)$$

Similarly to the procedure in one-leg supported phase, the inverse kinematics of the biped robot in two-leg supported phase can be obtained. It can be expressed as following equations.

$$h(k) = \sqrt{\frac{l_3^2}{4} + r^2(k) - l_3 y_{ca}(k)} \quad (71)$$

$$\alpha(k) = \angle BB_1B_2 = arccos\left(\frac{l_1^2 + l_2^2 - h^2(k)}{2l_1 l_2}\right) \quad (72)$$

$$\theta_3(k) = \pi - \alpha(k) \quad (73)$$

$$\theta_2(k) = \angle BB_2A = arcsin\left(\frac{y_{ca}(k) - \frac{l_3}{2}}{h(k)}\right) \quad (74)$$

$$\theta_1(k) = \angle DB_2B + \angle BB_2B_1 = arcsin\left(\frac{x_{ca}(k)}{h(k)}\right) + arccos\left(\frac{h^2(k) + l_1^2 - l_2^2}{2h(k)l_1}\right) \quad (75)$$

$$h_1(k) = \sqrt{\frac{l_3^2}{4} + r_1^2(k) - l_3 |y_{cf}(k)|} \quad (76)$$

$$\alpha_1(k) = \angle KK_1E = arccos\left(\frac{l_5^2 + l_4^2 - h_1^2(k)}{2l_5 l_4}\right) \quad (77)$$

$$\theta_8(k) = \pi - \alpha_1(k) \quad (78)$$

$$\theta_9(k) = \angle KEK_2 = arcsin\left(\frac{y_{cf}(k) + \frac{l_3}{2}}{h_1(k)}\right) \quad (79)$$

$$\theta_{10}(k) = \angle KEK_1 + \angle KEK_3 = arccos\left(\frac{h_1^2(k) + l_5^2 - l_4^2}{2h_1(k)l_5}\right) + arcsin\left(\frac{x_{cf}(k)}{h_1(k)}\right) \quad (80)$$

where h and h_1 are distance between right hip joint and ankle of right and left legs.

4.2 Control of the biped robot

Considering one step walking of the biped robot is illustrated by consequent movement as shown in Fig. 12. At the beginning of walking step, the left leg leaves the ground to start swinging. This leg swings with following a reference trajectory. During the swing of the left leg, the ZMP of the biped robot exists at the geometry center of the right foot. At the end of swinging, the left leg is contacted on the ground, and the biped robot is supported by two legs.

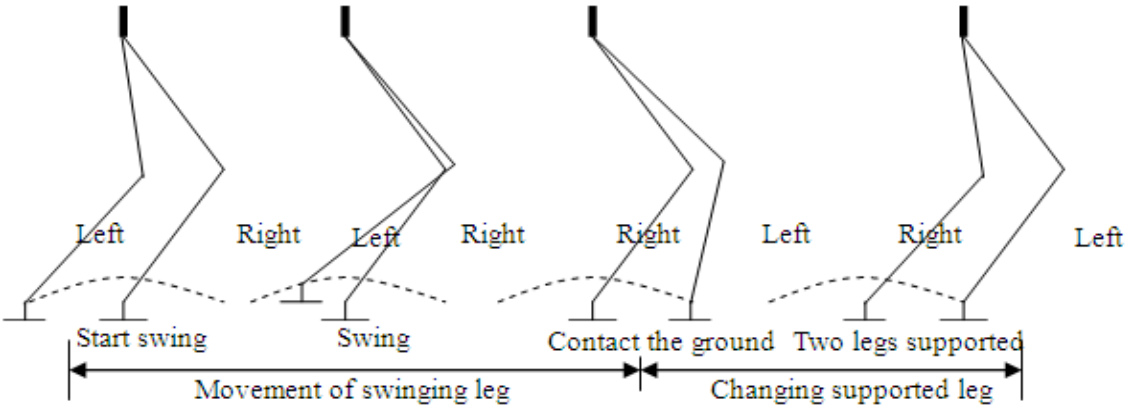

Fig. 12: One step walking of biped robot.

During two-leg supported phase, the ZMP of the biped robot moves from geometry center of the right foot to that of left foot. The left leg becomes new supported leg and the right leg becomes swinging leg for next step. Based on the reference trajectory of swinging leg and the trajectory of COM which is generated by ZMP servo system, the inverse kinematics is solved to obtain the angle of each joint of the biped robot. The control problem of biped robot becomes tracking control problem of DC motors of joints. The block diagram of the biped robot control system is shown in Fig. 13.

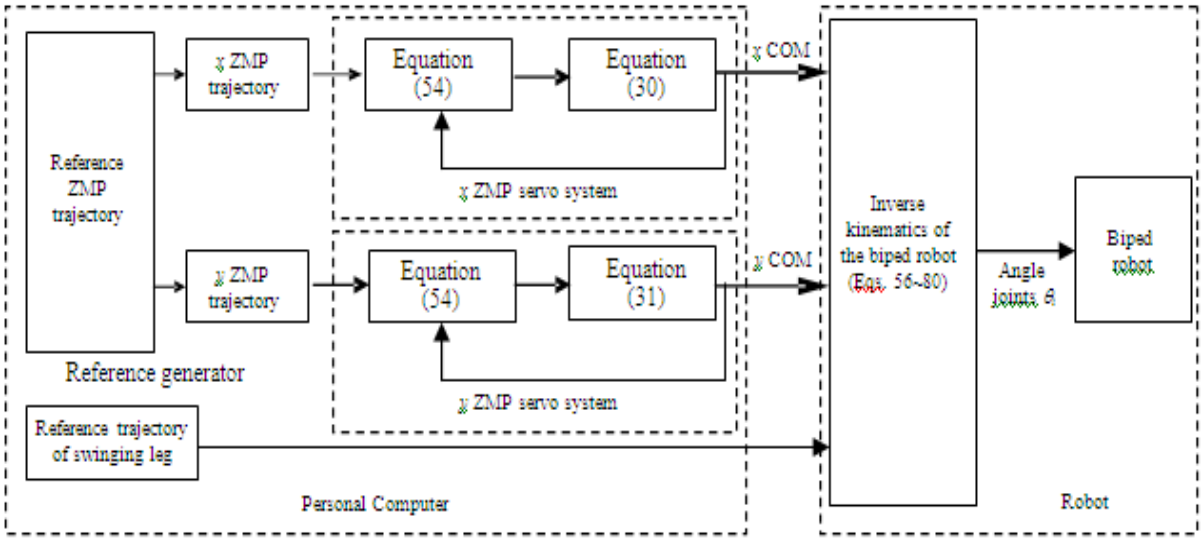

Fig. 13: Block diagram of the biped control system.

V. SIMULATION AND EXPERIMENTAL RESULTS

5.1 Hardware of the Biped Robot

The walking control method proposed in previous sections is implemented in CIMEC-1 developed for this paper as shown in Fig. 14.

Fig. 14: CIMEC-1 biped robot.

A simple hardware configuration using three PIC18F4431 and one dsPIC30F6014 for CIMEC-1 is shown in Fig. 15.

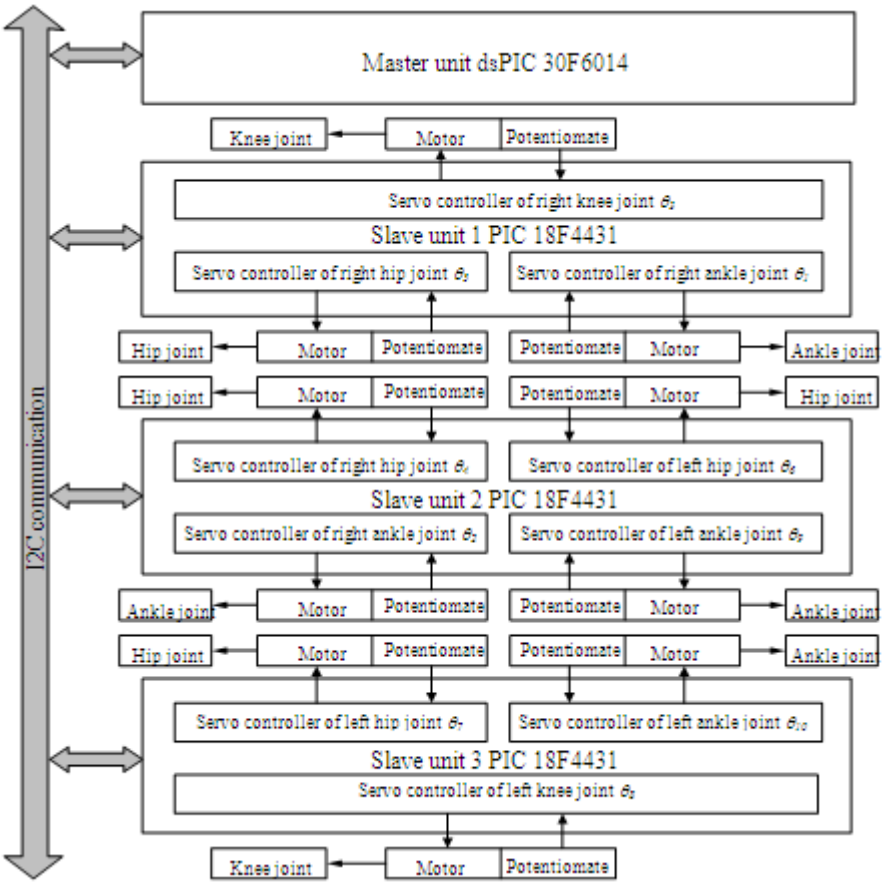

Fig. 15: Hardware configuration of the CIMEC-1.

dsPIC30F6014 is used as master unit, and PIC18F4431 is used as slave unit. The master unit and slave units communicate each other via I2C communication. The master unit is used to solve the inverse kinematics problem based on the trajectory of the center of the pelvis of the biped robot and trajectory of the ankle of swinging leg which are contained in its memory. It can also communicate personal computer via RS-232 communication. The angles at the k^{th} sample time obtained from inverse kinematics are sent to slave units as reference signals.

5.2 Simulation and experimental results

To demonstrate the performance of the biped walking based on the ZMP walking pattern generation combined with the inverse kinematics, the simulation results for walking on the flat floor of the biped robot using Matlab are shown. The period of step is 10 seconds: changing supported leg time is 5 seconds and swinging leg time is 5 seconds. The length of step is 20 cm. During the moving of the biped robot, the height of the center of pelvis link is constant. In the one-leg supported phase, ZMP is located at the center of the supported foot. When two legs of the biped robot are contacted on the ground, the ZMP moves from center of foot of current supported leg to the center of foot of the new supported leg.
The parameters values of the biped robot used in the simulation and experiment are given in Table 4.1.

Table 4.1 Numerical values of the biped robot' parameters used in simulation and experiment

Parameters	Description	Values	Units
$l_1 = l_5$	Length of lower leg links	0.28	[m]
$l_2 = l_4$	Length of upper leg links	0.28	[m]
l_3	Length of pelvis link	0.2	[m]
a	Width of foot	0.18	[m]
b	Length of foot	0.24	[m]
z_{cd}	Height of center of pelvis link	0.5	[m]

θ_{01}	Initial value of θ_1	26.75	[deg]
θ_{02}	Initial value of θ_2	0	[deg]
θ_{03}	Initial value of θ_3	53.5	[deg]
θ_{04}	Initial value of θ_4	0	[deg]
θ_{05}	Initial value of θ_5	26.75	[deg]
θ_{06}	Initial value of θ_6	0	[deg]
θ_{07}	Initial value of θ_7	26.75	[deg]
θ_{08}	Initial value of θ_8	53.5	[deg]
θ_{09}	Initial value of θ_9	0	[deg]
θ_{010}	Initial value of θ_{10}	26.75	[deg]

The footprint and the Zigzag reference trajectory of ZMP are shown in Fig. 16.

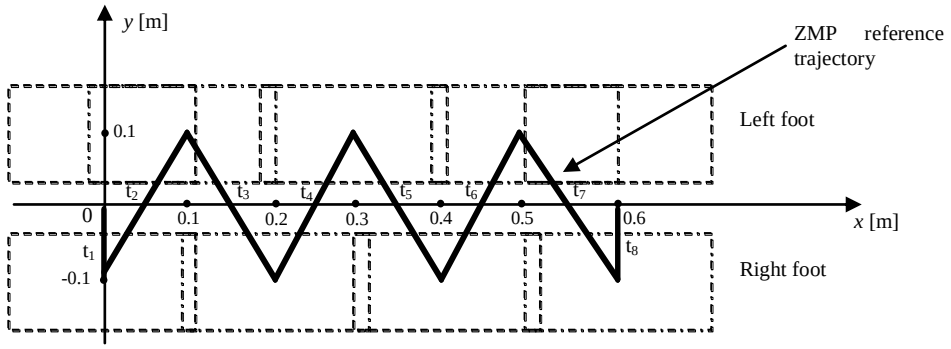

Fig. 16: Footprint and zigzag reference trajectory of ZMP.

The *x* and *y* ZMP trajectories versus times corresponding to the zigzag reference trajectory of ZMP in Fig. 16 can be obtained as shown in Fig. 17.

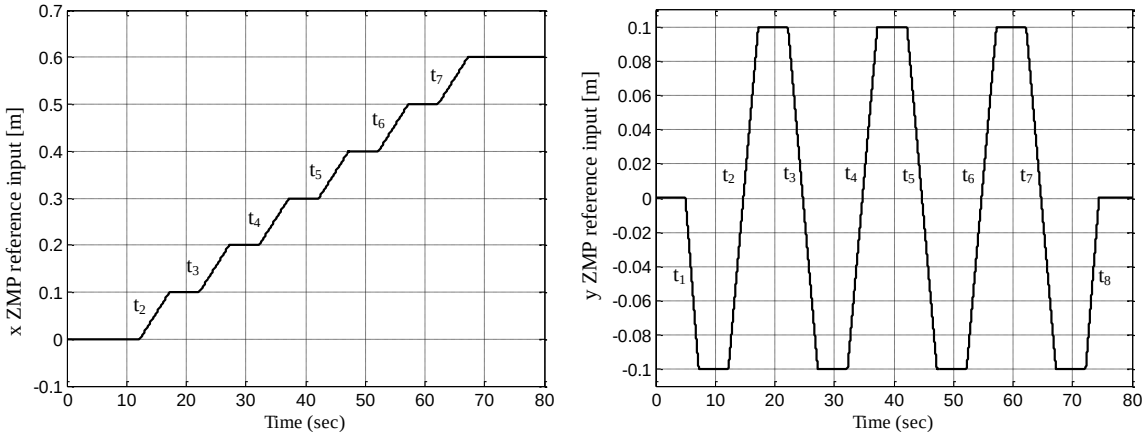

(a) *x* ZMP reference input versus time. (b) *y* ZMP reference input versus time.

Fig. 17: Zigzag ZMP reference input trajectory versus time.

The reference input trajectory of the ankle joint of swinging leg is an arc which has radius equal to 0.1 [m]. The reference input trajectory equations of arc are expressed as Eq. (81) for left leg and Eq. (82) for right leg.

$$\begin{cases} x_{aa}^2 + z_{aa}^2 = 0.01 \\ y_{aa} = l_3 \end{cases} \quad for \quad -0.1 \le x_{aa} \le 0.1 \quad (81)$$

$$\begin{cases} x_{af}^2 + z_{af}^2 = 0.01 \\ y_{af} = l_3 \end{cases} \quad for \quad -0.1 \le x_{af} \le 0.1 \quad (82)$$

where (x_{aa}, y_{aa}, z_{aa}) is coordinate of the point on the arc in the coordinate system Σ_a, and (x_{af}, y_{af}, z_{af}) is coordinate of the point on the arc in the coordinate system Σ_f.

The *x*, *y* ZMP servo control systems (30) and (31) are sampled with sampling time T = 1 [ms] and controlled by discrete time optimal tracking controller with $R = 1$, $Q = \left[\begin{array}{c|c} 0.12 & \boldsymbol{0} \\ \hline \boldsymbol{0} & \boldsymbol{0} \end{array}\right]$ and number of sample time in future of reference input $N = 1200$. The simulation and experimental results are shown in Figs. 18~27. Fig. 18 and Fig. 20 show the ZMP reference inputs, outputs and positions of the COM in *x* and *y* directions with respect to time. Fig. 19 and Fig. 21 show that the tracking errors of *x* and *y* ZMP servo systems converge to zeros and the errors at the transition points of reference inputs are very small. Figs. 22~26 show angles of each joint of the biped robot. In these figures, the sharp points occur at the transition states of the biped robot where joints of the biped robot change its direction of rotation. The movement of the COM of the biped robot is shown in Fig. 27.

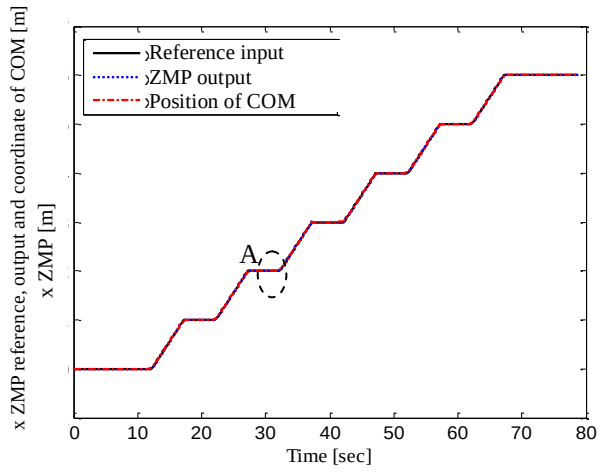

(a)

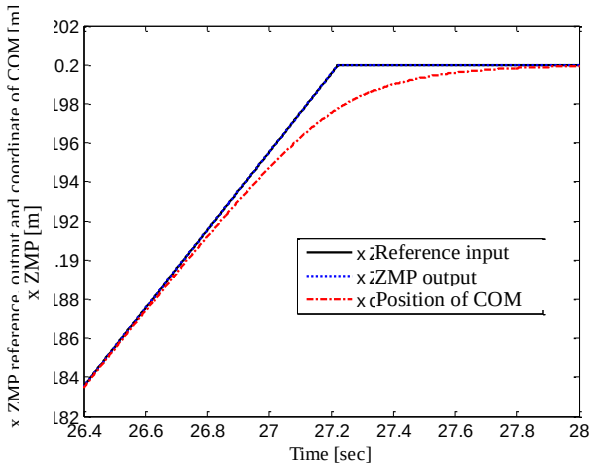

(b) A region.

Fig. 18: *x* ZMP reference input, *x* ZMP output and position of COM.

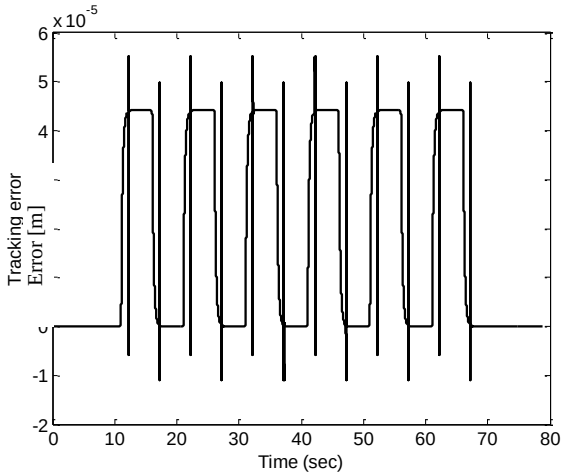

Fig. 19: *x* ZMP position error.

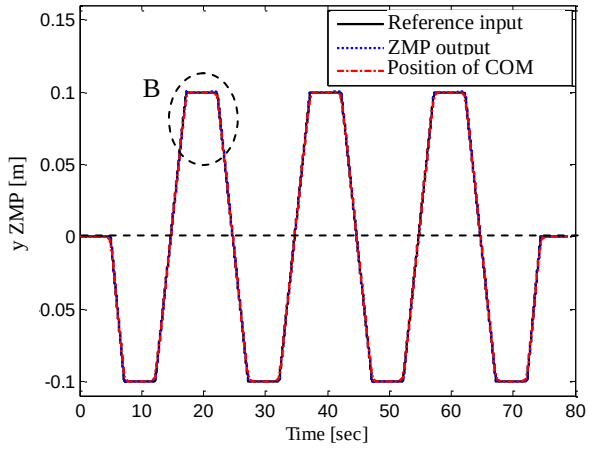

(a)

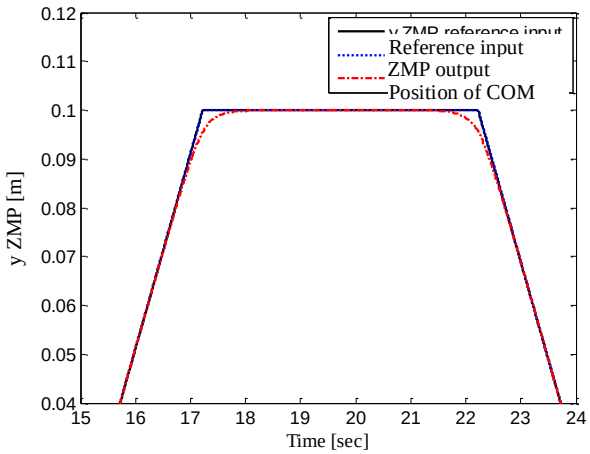

(b) B region.

Fig. 20: *y* ZMP reference input, *y* ZMP output and position of COM.

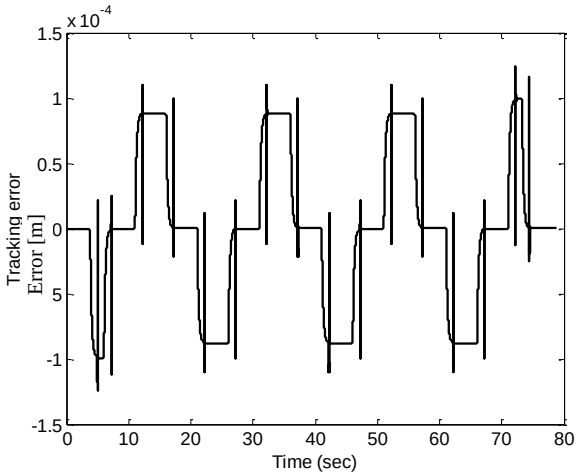

Fig. 21: *y* ZMP position error.

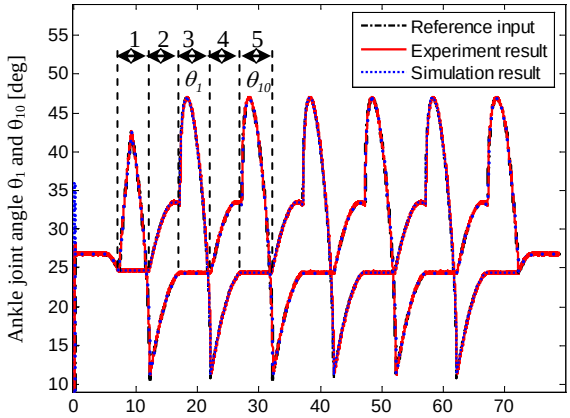

1: Supported leg.
2: Change supported leg.
3: Swing leg.
4: Change supported leg.
5: Supported leg.

Fig. 22: Simulation and experimental results of ankle joints angle θ_1 and θ_{10}.

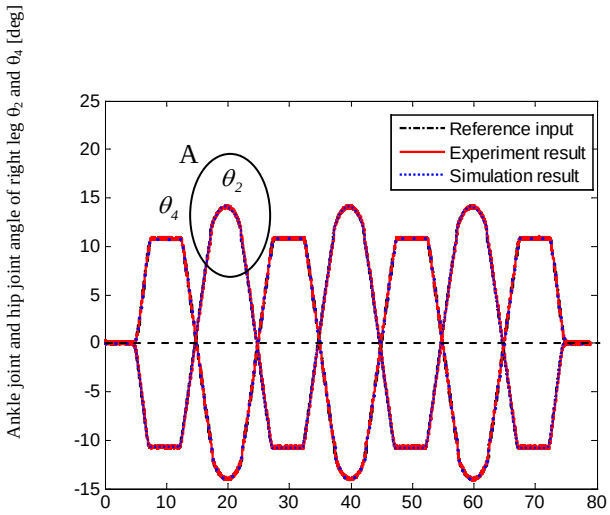

a)

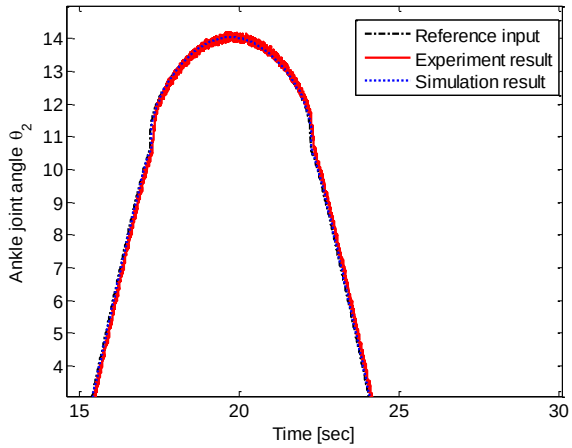

b) A region.

Fig. 23: Simulation and experimental results of ankle and hip joints angle θ_2 and θ_4.

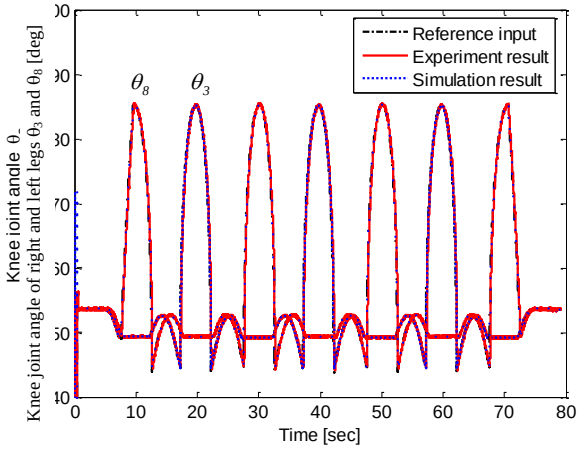

Fig. 24: Simulation and experimental results of knee joints angle θ_3 and θ_8.

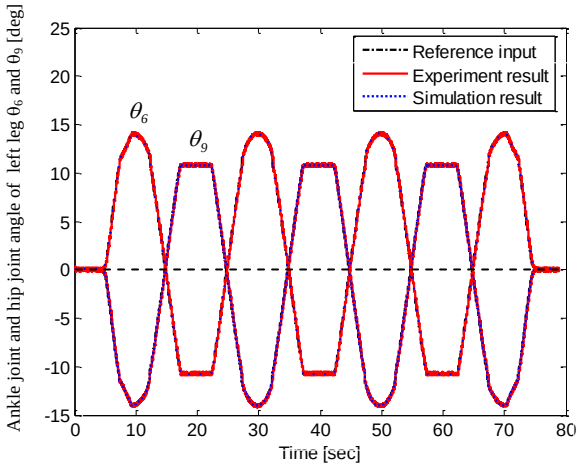

Fig. 25: Simulation and experimental results of hip and ankle joints angle θ_6 and θ_9.

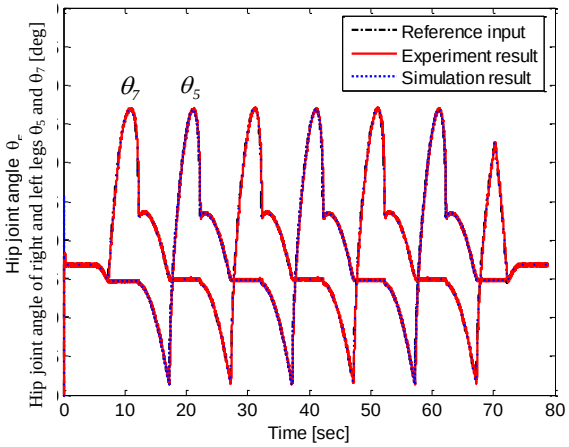

Fig. 26: Simulation and experimental results of hip joints angle θ_5 and θ_7.

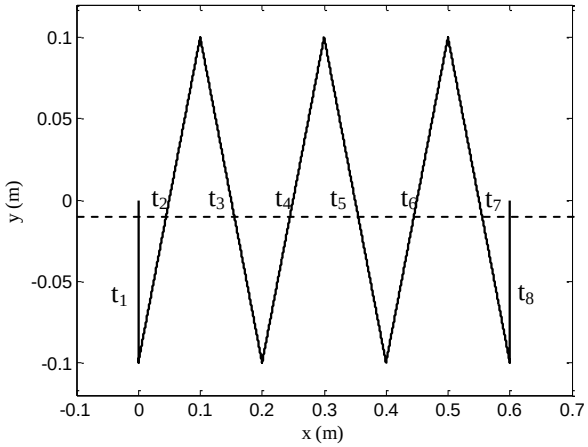

Fig. 27: Movement of the center of pelvis link.

VI. CONCLUSIONS

In this paper, a 10 DOF biped robot is developed. The kinematics and dynamic model of the biped robot are presented. For the stable walking, a controller using the discrete time optimal theory is designed to generate the trajectory of COM. The walking control of biped robot is performed based on the solutions of the inverse kinematics which is solved by solid geometry method. A simple hardware configuration is constructed to control for biped robot. The simulation and experimental results are shown to prove effectiveness of proposed controller.

REFERENCES

[1] S. Kajita, F. Kanehiro, K. Kaneko, K, Yokoi and H. Hirukawa, 2001, "The 3D Linear Inverted Pendulum Mode: A simple modeling for a biped walking pattern generation", Proc. of IEEE/RSJ International conference on Intelligent Robots and Systems, pp. 239~246.

[2] C. Zhu and A. Kawamara, 2003, "Walking Principle Analysis for Biped Robot with ZMP Concept, Friction Constraint, and Inverted Pendulum Model", Proc. of IEEE/RSJ International conference on Intelligent Robots and Systems, pp. 364~369.

[3] S. K. Agrawal, and A. Fattah, 2006, "Motion Control of a Novel Planar Biped with Nearly Linear Dynamics", IEEE/ASME Trans. Mechatronics, Vol. 11, No. 2, pp. 162~168.

[4] J. H. Part, 2001, "Impedance Control for Biped Robot Locomotion", IEEE Trans. Robotics and Automation, Vol. 17, No. 3, pp. 870~882.

[5] Q. Huang and Y. Nakamura, 2005, "Sensor Reflex Control for Humanoid Walking", IEEE Trans. Robotics, Vol. 21, No. 5, pp. 977~984.

[6] B. C. Kou, 1992, "Digital Control Systems", International Edition.

[7] D. Li, D. Zhou, Z. Hu, and H. Hu, 2001, "Optimal Priview Control Applied to Terrain Following Flight", Proc. of IEEE Conference on Decision and Control, pp. 211~216.

[8] C. Zhu and A. Kawamara, 2003, "Walking Principle Analysis for Biped Robot with ZMP Concept,

Friction Constraint, and Inverted Pendulum Model", Proc. of IEEE/RSJ International conference on Intelligent Robots and Systems, pp. 364~369.
[9] D. Plestan, J. W. Grizzle, E. R. Westervelt and G. Abba, 2003, "Stable Walking of A 7-DOF Biped Robot", IEEE Trans. on Robotics and Automation, Vol. 19, No. 4, pp. 653-668.
[10] F. L. Lewis, C. T. Abdallah and D.M. Dawson, 1993, "Control of Robot Manipulator", Prentice Hall International Edition.
[11] G. F. Franklin, J. D. Powell and A. E. Naeini, "Feedback Control of Dynamic System", Prentice Hall Upper Saddle River, New Jersey 07458.
[12] G. A. Bekey, 2005, "Autonomous Robots From Biological Inspiration to Implementation and Control", The MIT Press.
[13] H. K. Lum, M. Zribi and Y. C. Soh, 1999, "Planning and Control of a Biped Robot", Int. Journal of Engineering Science ELSEVIER, Vol. 37, pp. 1319~1349.
[14] H. Hirukawa, S. Kajita, F. Kanehiro, K. Kaneko and T. Isozumi, 2005, "The Human-size Humanoid Robot That Can Walk, Lie Down and Get Up", International Journal of Robotics Research, Vol. 24, No. 9, pp. 755~769.
[15] K. Mitobe, G. Capi and Y. Nasu, 2004, "A New Control Method for Walking Robots Based on Angular Momentum", Journal of Mechatronics ELSEVIER, Vol. 14, pp. 164~165.
[16] K. Harada, S. Kajita, K. Kaneko and H. Hirukawa, 2004, "Walking Motion for Pushing Manipulation by a Humanoid Robot", Journal of the Robotics Society of Japan, Vol. 22, No. 3, pp. 392–399.